

UNCLASSIFIED

AD NUMBER

AD304831

CLASSIFICATION CHANGES

TO: unclassified

FROM: confidential

LIMITATION CHANGES

TO:  
Approved for public release; distribution is unlimited.

FROM:  
Distribution authorized to U.S. Gov't. agencies only; Foreign Government Information; JUL 1958. Other requests shall be referred to British Embassy, 3100 Massachusetts Avenue, NW, Washington, DC 20008.

AUTHORITY

DSTL, AVIA 6/20574, 18 Nov 2008; DSTL, AVIA 6/20574, 18 Nov 2008

THIS PAGE IS UNCLASSIFIED

14

**CONFIDENTIAL**

FWE-231

This document consists of 22 pages  
No. 18 of 200 copies, Series TA

US  
[REDACTED]  
[REDACTED]  
[REDACTED]  
[REDACTED]

# **FOREIGN WEAPON EFFECTS REPORTS**

*... received under the Technical Cooperation Program*

**THE EFFECTS OF NON-UNIFORM ABSORBTIVITY  
OF THERMAL RADIATION FROM NUCLEAR  
EXPLOSIONS ON THE TEMPERATURE RISE  
IN AN AIRCRAFT SKIN**

TIS Issuance Date: September 21, 1959

This material contains information affecting the national defense of the United States within the meaning of the espionage laws Title 18, U. S. C., Secs. 793 and 794, the transmission or revelation of which in any manner to an unauthorized person is prohibited by law.

**UNITED STATES ATOMIC ENERGY COMMISSION**

**CONFIDENTIAL**



When no longer required, this document may be destroyed in accordance with applicable security regulations.

**DO NOT RETURN THIS DOCUMENT**

**CONFIDENTIAL**

AD-304831

**ROYAL AIRCRAFT ESTABLISHMENT**

**Farnborough, England**

**RAE-Technical Note Mech. Eng. 268**

**THE EFFECTS OF NON-UNIFORM ABSORBTIVITY OF  
THERMAL RADIATION FROM NUCLEAR EXPLOSIONS  
ON THE TEMPERATURE RISE IN AN  
AIRCRAFT SKIN**

**B. J. Brinkworth, M.Sc.**

**July 1958**

**This material contains information affecting  
the national defense of the United States  
within the meaning of the espionage laws  
Title 18, U. S. C., Secs. 793 and 794, the  
transmission or revelation of which in any  
manner to an unauthorized person is pro-  
hibited by law.**

**U. S. Atomic Energy Commission  
Technical Information Service**

**CONFIDENTIAL**

20080630 287

LIST OF CONTENTS

	<u>Page</u>
1 INTRODUCTION	5
2 THIN SKIN IRRADIATED THROUGH A LONG PARALLEL SLOT	6
2.1 Assumptions	6
2.2 Numerical analysis	7
2.3 Accuracy	9
2.4 Example	9
3 TEMPERATURE RISE UNDER INSIGNIA	10
3.1 Adaptation of previous analysis	10
3.2 Example	11
4 LIMITS OF VALIDITY OF THE GENERAL ANALYSIS	12
4.1 Effect of paints	12
4.2 Effect of shape	12
5 CONCLUSION	13
ACKNOWLEDGEMENT	13
NOTATION	14
LIST OF REFERENCES	15
ILLUSTRATIONS - Figs.1-5	16

LIST OF ILLUSTRATIONS

	<u>Fig.</u>
Nomenclature	1
Typical temperature distribution	2
Maximum temperature rise	3
Maximum temperature rise under insignia, $b = 0$	4
Maximum temperature rise under insignia, $b = 0.08$	5



# CONFIDENTIAL

## THE EFFECTS OF NON-UNIFORM ABSORBTIVITY OF THERMAL RADIATION FROM NUCLEAR EXPLOSIONS ON THE TEMPERATURE RISE IN AN AIRCRAFT SKIN

### SUMMARY

An analysis is made of the maximum temperature rise in a thin sheet exposed over a long narrow area to thermal radiation from a nuclear explosion. The study is extended to cases in which heat is absorbed outside this area to a lesser degree than inside it.

The results are applied to the temperature rise in aircraft skins subject to aerodynamic cooling and irradiated through rectangular apertures, and also to the effects of the non-uniform absorbtivity where there are insignia.

It is shown that the effects of conduction to lesser-irradiated areas are substantial, and that the temperature rise in areas under insignia is less than would be expected from their greater absorbtivity.

### 1 INTRODUCTION

The effects on aircraft in flight of thermal radiation from nuclear explosions pose some unique problems in transient thermal conduction. In a previous study<sup>1</sup>, the influence of convective cooling by the airstream on the temperature rise in thin skins was determined for situations in which the skin was uniformly irradiated. It was assumed that the region being studied was not affected by conduction of heat to other parts of the structure, though this could clearly have an important effect in many situations, and requires further study.

Perhaps the most elementary instance of conduction to another part of the structure occurs when the skin is only partly, or non-uniformly, irradiated, and heat is transferred to another part of the skin itself. Practical situations of this kind arise when, for example, thermal radiation passes through an aperture and falls on a small area of an internal surface. Sometimes the irradiated area is exposed to the airstream, so that heat is lost both to the surrounding material and to the air.

Another, and commoner instance concerns the temperature rise in the part of a skin beneath insignia having a higher absorbtivity than the

surrounding reflective finish. Again, heat is lost both to the adjacent parts of the skin and to the airstream. These two situations are very similar, and differ only in that the surrounding material is also irradiated in the case of areas under insignia.

These particular situations are studied in the present Note, using a generalised analysis so that the results can be expressed in non-dimensional form, covering a range of the variables relating to the majority of practical cases. To avoid unnecessary repetition, it is assumed that the characteristics of the thermal input pulse from a nuclear explosion and certain aspects of the numerical analysis used are familiar to the reader. Reference may be made, if necessary, to the earlier study<sup>1</sup>.

## 2 THIN SKIN IRRADIATED THROUGH A LONG PARALLEL SLOT

### 2.1 Assumptions

The situation studied concerns a thin skin irradiated through a long parallel slot and cooled on one side by an airstream. In a general analysis, the following assumptions are necessary, though they may nearly all be discarded if a particular situation having special characteristics is being studied.

- (a) The heat transfer coefficient between skin and boundary layer is constant.
- (b) The thermal properties of the skin are constant.
- (c) The reflectivity of the surface is constant.
- (d) The skin and boundary layer temperatures are initially equal.
- (e) There are no temperature gradients through the skin.
- (f) There is no heat loss by re-radiation.

A simple numerical analysis will be used, in which the skin will be divided into discrete elements of width  $\Delta x$ , and time into intervals  $\Delta t$ . Fig.1 illustrates the nomenclature used. It will be further assumed that

- (g) The rate of heat input is uniform over the irradiated area and is zero beyond it (i.e., the aperture is very close to the skin or the radiation is collimated).
- (h) The heat transfer process is one-dimensional (i.e., the aperture is long enough for the temperatures to be uniform in the lengthwise direction).
- (i) The temperature of an element is defined by the temperature at its centre.
- (j) Heat is transferred internally only between adjacent elements.
- (k) The total heat input during a time interval is absorbed instantaneously at the beginning of the interval, raising the temperature accordingly.
- (l) The temperature distribution relaxes during an interval by heat transfer to the airstream and the adjacent material at a rate determined by the temperatures at the beginning of the interval.



## 2.2 Numerical analysis

Consider the rise in temperature in the nth element, (Fig.1) assumed to be of unit length perpendicular to the paper, and at a temperature  $T_n$  above that of the boundary layer at the beginning of a typical time interval.

The nett heat input during a time interval  $\Delta t$  is

$$P(t) \Delta x \Delta t - h T_n \Delta x \Delta t + (T_{n-1} - T_n) \frac{k\ell\Delta t}{\Delta x} + (T_{n+1} - T_n) \frac{k\ell\Delta t}{\Delta x} \quad (1)$$

(if  $n > r$ ,  $P(t) = 0$ ).

At the end of the interval, the temperature rise will have increased to  $T'_n$ , so that the total heat retained will be

$$zc\ell \Delta x (T'_n - T_n) \quad (2)$$

and (1) and (2) are equal.

Multiplying (1) and (2) by  $\frac{\Delta x}{k\ell\Delta t}$  and equating, we have

$$\frac{P(t) (\Delta x)^2}{k\ell} - \frac{h (\Delta x)^2}{k\ell} \cdot T_n + (T_{n-1} - T_n) + (T_{n+1} - T_n) = \frac{zc (\Delta x)^2}{k\Delta t} (T'_n - T_n) \quad (3)$$

Now if 
$$\frac{zc (\Delta x)^2}{k\Delta t} = M \quad (4)$$

equation (3) may be re-arranged thus:-

$$\frac{P(t)(\Delta t)}{zc\ell} - \frac{h \Delta t}{zc\ell} \cdot T_n + \frac{T_{n-1} + (M-2) T_n + T_{n+1}}{M} = T'_n \quad (5)$$

Let  $P(t) \Delta t = \Delta Q(t)$ , the total heat input per unit area during the interval, and make the substitutions

$$\Delta Q(t) = \frac{\Delta Q(t)}{Q} \cdot Q \quad (6)$$

$$\frac{Q}{zc\ell} = T_i \quad (7)$$

$$\Delta t = \frac{\Delta t}{t_{\max}} \cdot t_{\max} \quad (8)$$

and 
$$\frac{ht_{\max}}{zc\ell} = b \text{ (see ref 1)} \quad (9)$$



Then equation (5) becomes

$$\frac{\Delta Q(t)}{Q} \cdot T_i - b \cdot \frac{\Delta t}{t_{\max}} \cdot T_n + \frac{T_{n-1} + (M-2) T_n + T_{n+1}}{M} = T'_n \quad (10)$$

Now  $T_i$  is the "ideal" temperature rise which would result if the entire heat input were absorbed. Dividing each term by  $T_i$ , we may introduce a non-dimensional temperature rise scale in which

$$\frac{T}{T_i} = \Gamma \quad (11)$$

Then equation (10) becomes

$$\frac{\Delta Q(t)}{Q} - b \cdot \frac{\Delta t}{t_{\max}} \cdot \Gamma_n + \frac{\Gamma_{n-1} + (M-2) \Gamma_n + \Gamma_{n+1}}{M} = \Gamma'_n \quad (12)$$

Thus, the temperature rise in a given element at the end of a time interval may be determined numerically from the temperature rise in that element and its immediate neighbours at the beginning of the interval. The computational effort involved depends on the value of  $M$ , which may be chosen arbitrarily so long as it is greater than 2. If  $M$  equalled 2, the temperature of an element would not depend on its previous history, and if  $M$  were less than 2, the previous history would have a negative effect on the temperature rise, which is unreal physically. It is very convenient, in practice, to make  $M = 3$ , since then the numerical work merely involves averaging the initial temperatures. Equation (12) then becomes

$$\frac{\Delta Q(t)}{Q} - b \cdot \frac{\Delta t}{t_{\max}} \cdot \Gamma_n + \frac{\Gamma_{n-1} + \Gamma_n + \Gamma_{n+1}}{3} = \Gamma'_n \quad (13)$$

which can be evaluated so long as  $\frac{\Delta Q(t)}{Q}$  is known as a function of  $\frac{t}{t_{\max}}$ .

In making  $M = 3$ , certain other factors are also determined, since

$$\begin{aligned} M &= \frac{zc(\Delta x)^2}{k\Delta t} \\ &= \frac{zcL^2}{k t_{\max}} \cdot \left(\frac{\Delta x}{L}\right)^2 \cdot \frac{t_{\max}}{\Delta t} \end{aligned}$$

The function  $\frac{zcL^2}{k t_{\max}}$  is a characteristic parameter, so let

$$B = \frac{zcL^2}{k t_{\max}} \quad (14)$$

Then 
$$M = B \cdot \left(\frac{\Delta x}{L}\right)^2 \cdot \frac{t_{\max}}{\Delta t} \quad (15)$$

The non-dimensional temperature distribution has been computed for  $2 < B < 200$  and  $b = 0, 0.04$  and  $0.08$ , which embraces the majority of practical situations. In the analysis used,  $M$  was always 3, and the number of material elements and time intervals were chosen to satisfy equation (15).

The smallest number of elements used was  $\frac{L}{\Delta x} = 5$ ; odd numbers were used so that an element coincided with the centreline, which is a centre of symmetry.

Fig.2 illustrates a typical variation of temperature rise with time, showing how the heat spreads out into the adjacent non-irradiated skin. In this example, the distribution after the maximum is not shown, to avoid confusion of the diagram.

The maximum temperature rise occurs at the centre of the irradiated area, and this is plotted in Fig.3 in non-dimensional form.

### 2.3 Accuracy

In using a finite difference analysis, the accuracy achieved depends on the number of elements of space and time employed, and it is often difficult to assess the accuracy without repeating the computations with more elements and comparing the solutions. In this particular situation, however, an analytical solution exists for the special case of a constant rate of heat input and no air cooling<sup>2</sup> ( $b = 0$ ). This solution, using the present notation, is

$$\Gamma_m = \frac{2}{\sqrt{\pi}} X e^{-X^2} + \operatorname{erf}(X) - 2X^2 \operatorname{erfc}(X) \quad (16)$$

where 
$$X^2 = \frac{zcL^2}{16 k t_h} \quad (17)$$

and  $t_h$  is the total heating time.

The present method was used with  $\frac{L}{\Delta x} = 5$  and  $M = 3$  for  $X = 0.485$  and  $0.685$  and the comparative solutions obtained for  $\Gamma_m$  were:-

Numerical	0.694	0.824
Analytical	0.708	0.838

The error in both cases was less than 2%, from which it is concluded that the results of the previous analysis should not be less accurate. The errors involved in applying the results to real situations are clearly likely to be much greater than the computational errors.

### 2.4 Example

In the previous study<sup>1</sup>, an example was considered in which a bomber aircraft was exposed to thermal radiation from a 2Mt explosion when flying straight and level at a Mach number of 0.8 at 45,000 ft. The convective heat transfer coefficient at a point 12 ft downstream from the wing leading edge was found to be

$$h = 1.61 \times 10^{-3} \text{ cal cm}^{-2} \text{ sec}^{-1} \text{ } ^\circ\text{C}^{-1}$$



and for a 26 gauge skin in DTD 546 material this gave

$$b = 0.088$$

Now suppose that this part of the skin was in the upper surface of the wing and had been irradiated through an aperture over a rectangular area  $L = 2$  cm wide, and the total thermal dose was  $Q = 10$  cal $\text{cm}^{-2}$  after correction for obliquity of the surface and its reflectivity.

$$\text{For DTD 546, } k = 0.27 \text{ cal}\text{cm}^{-1} \text{ sec}^{-1} \text{ } ^\circ\text{C}^{-1}$$

$$z = 2.79 \text{ gr cm}^{-3}$$

$$\text{and } c = 0.21 \text{ cal}\text{gr}^{-1} \text{ } ^\circ\text{C}^{-1}$$

$$\text{so that } \frac{k}{zc} = 0.46 \text{ cm}^2 \text{ sec}^{-1}$$

$$\text{and if } L = 2 \text{ cm}$$

$$\text{and } t_{\text{max}} = 1.43 \text{ secs,}$$

$$B = 6.1,$$

from equation (14)

Then from Fig.3

$$\Gamma_m = 0.35$$

(It is evident that, in this case, convective cooling to the airstream is very small compared with the heat transfer to the surrounding material).

From equation (6),

$$T_i = 381^\circ\text{C}$$

$$\text{and thus } T_m = 132^\circ\text{C}$$

Then if the assumptions of section 2.1 are valid, the maximum temperature rise is  $132^\circ\text{C}$ .

### 3 TEMPERATURE RISE UNDER INSIGNIA

#### 3.1 Adaptation of previous analysis

The identification letters and other insignia on a bomber aircraft cover considerable areas of the skin and have a higher absorbtivity than the surrounding finish. It is possible to use the previous analysis to determine the rise in temperature in the skin behind such insignia, if certain further assumptions are made. The validity of the analysis will be considered later.

For parts of insignia covering rectangular areas, the situation is only slightly different from the irradiation of a skin through a rectangular aperture. In the latter instance, there is no heat input beyond the edge of the irradiated area (i.e. if  $n > r$ ). If the input to the surrounding skin is  $P(t)$ , the effective input to the areas under insignia will be

$$P(t)_{\text{in}} = P(t) \frac{a_{\text{in}}}{a} \quad (18)$$

and correspondingly

$$\frac{\Delta Q(t)_{in}}{Q} = \frac{\Delta Q(t)}{Q} \cdot \frac{a_{in}}{a} \quad (19)$$

In this case,  $Q$  is the total thermal dose corrected for the obliquity and reflectivity of the plain skin. Then the maximum temperature rise is expressed in terms of the "ideal" temperature rise in the skin outside the insignia, which will be the  $T_i$  upon which the non-dimensional temperature  $\Gamma$  is based (vide equation (10)).

The variation of  $\Gamma_m$  with  $B$  and  $\frac{a_{in}}{a}$  is shown in Figs.4 and 5 for  $b = 0$  and  $b = 0.08$  respectively. It is indicated that the temperature rise under highly absorbing areas is substantially less than would be estimated from their absorbtivity only. This will be illustrated in the following example.

### 3.2 Example

The maximum temperature rise is required in the 16 gauge light-alloy skin beneath a black identification number (say number one, for convenience) 2 in. wide (5.1 cm) for which  $a_{in} = 1.0$ .

A total thermal dose of  $50 \text{ cal cm}^{-2}$  is incident normal to the surface, which is finished with a white reflective paint for which  $a = 0.2$ . The average heat transfer coefficient for the region gives  $b = 0.08$ , and the weapon yield (4Mt., say) gives  $t_{max} = 2.0$  secs.

$$\text{Now} \quad Q = 10 \text{ cal cm}^{-2}$$

$$\text{and hence} \quad T_i = 104^\circ\text{C}$$

for a 16 gauge skin in DTD 546.

$$\text{As before, } \frac{k}{zc} = 0.46 \text{ cm}^2 \text{ sec}^{-1}, \text{ so that, from equation (14)}$$

$$B = 28$$

$$\text{Also} \quad \frac{a_{in}}{a} = 5$$

Hence, from Fig.5,

$$\Gamma_m = 2.25$$

$$\text{and thus} \quad T_m = 234^\circ\text{C}$$

Therefore, the maximum temperature rise (in the centre of the number) would be  $234^\circ\text{C}$ . It might have been assumed, in making a first estimate of the maximum temperature rise, that there was no conduction to adjacent areas. The estimate would then be obtained by multiplying the temperature rise in the surrounding areas by  $\frac{a_{in}}{a}$ . From a previous analysis<sup>1</sup>, the maximum temperature rise in the white region would be  $0.57 T_i$ , so that the estimated maximum temperature rise in the black region would be  $2.85 T_i = 297^\circ\text{C}$ ., an over-estimate of about 30%.



The error in this simple approach becomes less for large values of B, but greater for small values of b. In the example given above, the value of b is too high for a typical situation, and had it been zero, for example, the error in the simple estimate would have been nearly 80%.

#### 4 LIMITS OF VALIDITY OF THE GENERAL ANALYSIS

##### 4.1 Effect of paints

On very thin skins, the heat capacity of any reflective finishes applied to the surface may be of the same order as that of the skin itself. This can be allowed for approximately, if the thickness and nature of the paint is constant and its thermal properties known. Then the heat capacity per unit area,  $zc_1$ , would be that of the combined skin and paint, though the thermal diffusivity  $\frac{k}{zc}$  would probably not be affected since most paints are poor conductors of heat.

When insignia are applied on top of the existing finish, the thickness and thermal properties of the paint within the area of the insignia are likely to be different from those of the surrounding finish. Such a case would have to be analysed individually, since the general analysis assumes constant properties throughout. This is not thought to be very important in view of the fact that most insignia are found on fairly thick skins, to whose heat capacity they would make a negligible contribution.

The presence of a paint film of low conductivity on the exposed surface may prevent the realisation of the assumed zero temperature gradient in the thickness direction. The significance of this cannot be assessed without greater knowledge of the thermal properties of typical finishes, but deserves further study.

##### 4.2 Effect of shape

One of the assumptions upon which the analysis rests is that there is no heat loss in the lengthwise direction, i.e. that the irradiated area is very long. It is valuable to determine how long it should be in practice for the error in using the results to be acceptable. The analysis itself can be used to indicate the order of the length required.

Suppose the length of the area is Y. Then from Fig.3, applied to heat flow in the lengthwise direction, the approach to zero heat flow ( $\Gamma_m = 1.0$ ) would depend upon the parameter

$$B^* = \frac{zc Y^2}{k t_{\max}} \quad (20)$$

Fig.3 does not extend beyond  $\Gamma_m = 0.76$  since this would require input data after  $t = 10 t_{\max}$ , which are not available. However, it is estimated that  $\Gamma_m$  would reach 0.9 (10% error) for  $B^* = 800$  and 0.95 (5% error) for  $B^* = 1700$ .

For most light alloys, the thermal diffusivity  $\frac{k}{zc}$  is of the order of  $0.5 \text{ cm}^2 \text{ sec}^{-1}$ , and for megaton weapons,  $t_{\max} = 1$  to 2 secs. Then it is indicated that under these circumstances, an irradiated area may be considered long if  $Y = 30 \text{ cm}$  (10% error) or  $40 \text{ cm}$  (5% error) approximately.

These lengths are smaller than those of the straight portions of most standard identification numbers<sup>3</sup> and it is considered to be legitimate to use the analysis for curved portions also. Furthermore, it is indicated that heat flow for one absorbing area would not be seriously affected by another one further away than  $Y/2$ , i.e. 20 cm, say, even for megaton explosions.

The temperature rise beneath roundels and other national emblems cannot be treated rigorously with the present method, although estimates should be possible which are not enormously in error. In this connection, and for the case of irradiation through a circular aperture, it is worth noting that the temperature rise at the centre of a circular area of diameter  $D$  must always be less than that in the centre of a long strip of width  $D$ . Then the value of  $T_m$  corresponding to  $B = \frac{zcD^2}{kt_{\max}}$  would always be a safe estimate.

## 5 CONCLUSION

A simple numerical analysis has been devised for computing the maximum temperature rise in a thin skin irradiated over a long narrow area, and extended to cases in which heat is absorbed outside this area to a lesser degree than inside it.

The results have been applied to the temperature rise in aircraft skins subject to aerodynamic cooling and irradiated through long apertures, and also to the effects of non-uniform absorbtivity where there are identification numbers and other insignia.

It is shown that the effects of conduction to non-irradiated or lesser-irradiated areas are substantial, and that the temperature rise in areas under insignia is less than would be expected from a consideration of their greater absorbtivity.

## ACKNOWLEDGEMENT

Nearly all the extensive numerical computation employed in this Note was carried out by Mr. D. J. Nosworthy of this Department.



## NOTATION

The symbols used are defined as follows:-

a	absorbitivity of surface
b	parameter $\frac{h t_{\max}}{z c \ell}$
B	parameter $\frac{z c L^2}{k t_{\max}}$
B*	parameter $\frac{z c Y^2}{k t_{\max}}$
c	specific heat of skin material
D	diameter of irradiated area
h	heat transfer coefficient between boundary layer and skin
k	thermal conductivity of skin material
$\ell$	thickness of skin
L	width of irradiated area
M	function $\frac{z c (\Delta x)^2}{k \Delta t}$
P(t)	thermal input per unit area per unit time
Q	total thermal dose per unit area $\times$ absorbitivity
$\Delta Q(t)$	thermal dose per unit area incident during interval $\Delta t$
t	time
$\Delta t$	interval of time
$t_{\max}$	time at which P(t) has maximum value
$t_h$	total heating time for square pulse
T	temperature rise above initial value
T'	temperature rise at end of time interval
$T_i$	"ideal" temperature rise $\frac{Q}{z c \ell}$
$T_m$	maximum temperature rise
$\Gamma$	non-dimensional temperature rise $\frac{T}{T_i}$
$\Gamma_m$	maximum value of $\Gamma = \frac{T_m}{T_i}$
$\Delta x$	width of space element

NOTATION (Contd)

- X parameter  $\left(\frac{z c L^2}{16 k t_h}\right)^{\frac{1}{2}}$   
Y length of irradiated area  
z density of skin material

SUBSCRIPTS

- n denotes typical space element  
r denotes last element before discontinuity boundary  
in denotes within discontinuity boundary

OPERATORS

erf(u) error function  $\frac{2}{\sqrt{\pi}} \int_0^u e^{-u^2} du$

erfc(u) complementary error function  $\frac{2}{\sqrt{\pi}} \int_u^{\infty} e^{-u^2} du$

---

LIST OF REFERENCES

<u>No.</u>	<u>Author(s)</u>	<u>Title, etc</u>
1	Brinkworth, B. J.	Skin temperature rise in an aircraft exposed to thermal radiation from a nuclear explosion. RAE Tech Note No. Mech Eng 251, March, 1958. Confidential.
2	Thomas, P. H.	The irradiation of thin sheets. JFRO Note No. 186/1955, June, 1955. Unclassified.
3	-	Design requirements for aircraft for the Royal Air Force and Royal Navy. Air Publication 970, vol.1. Restricted.



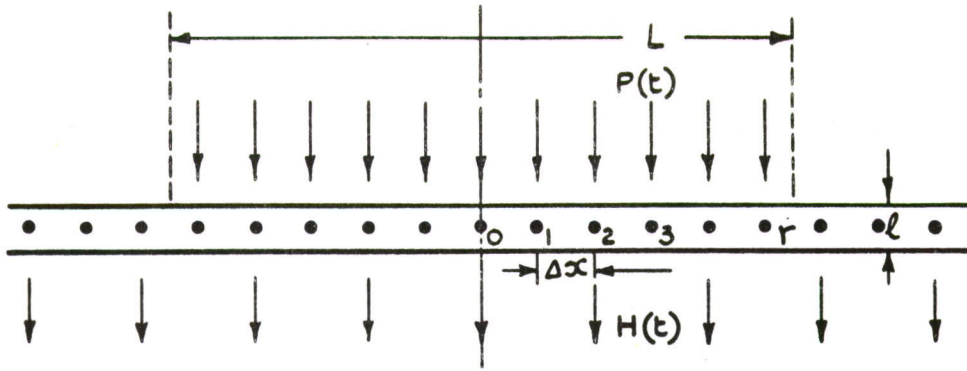


Fig. 1--Nomenclature.

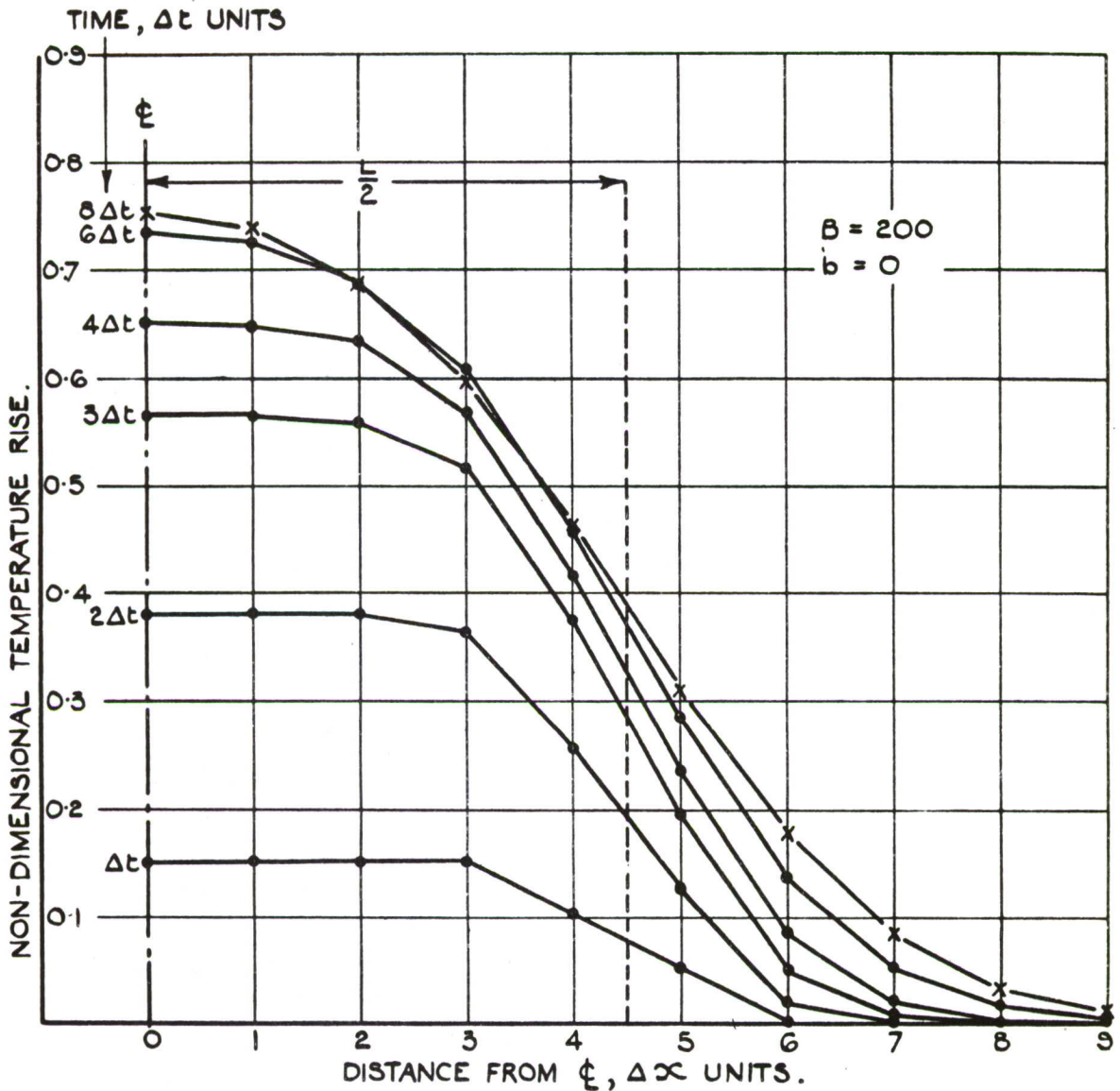


Fig. 2--Typical temperature distribution.

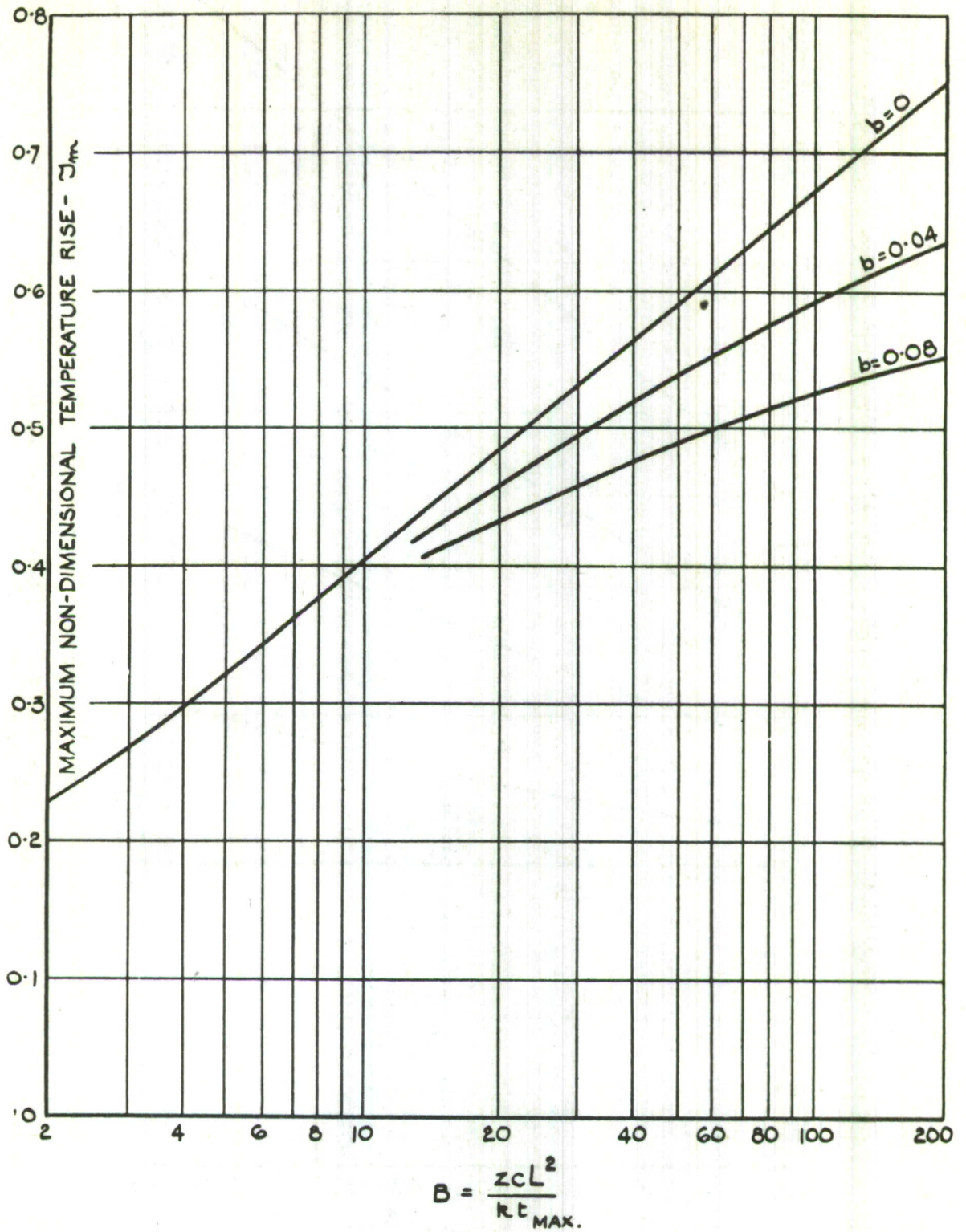


Fig. 3--Maximum temperature rise.



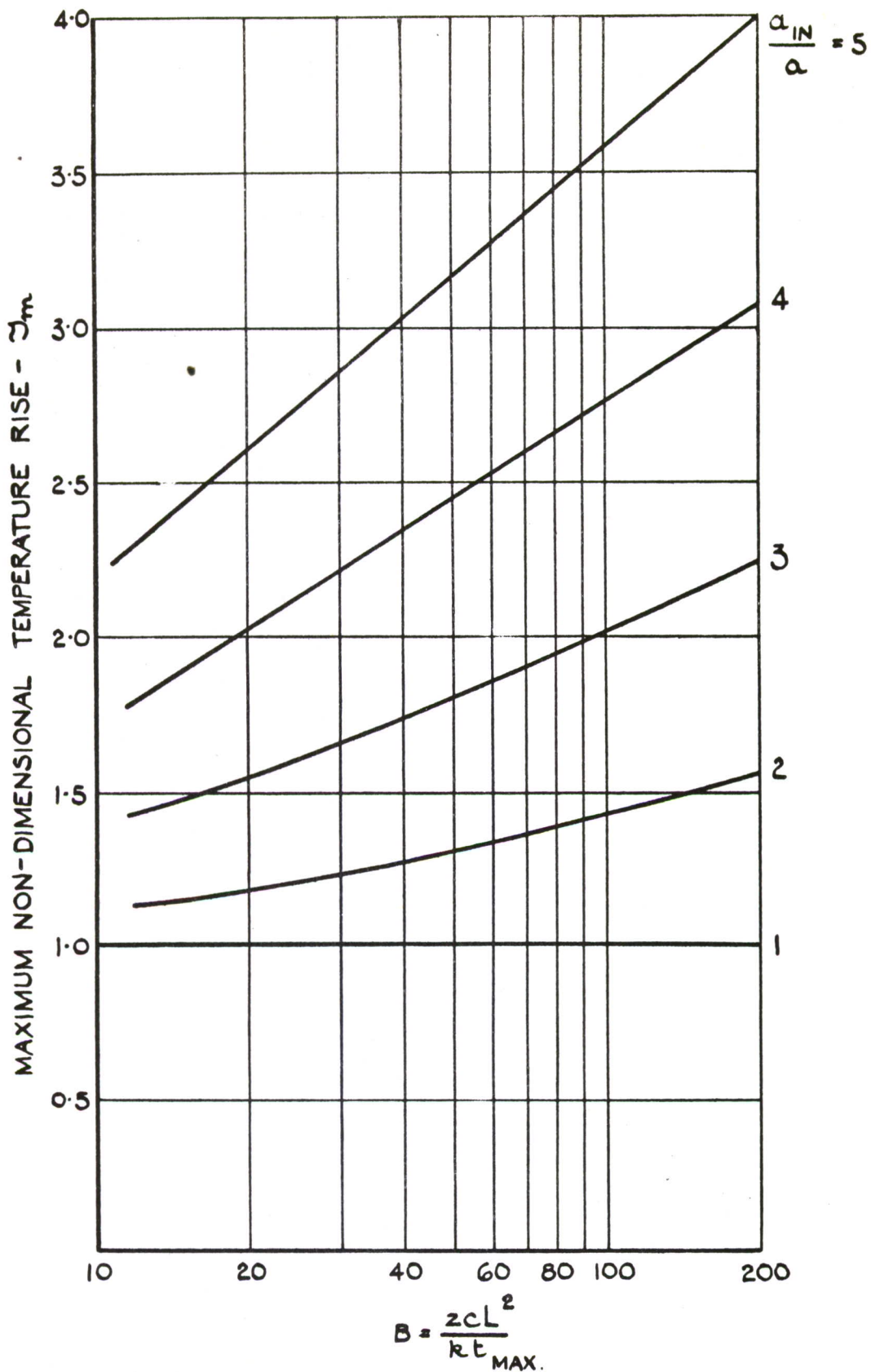


Fig. 4--Maximum temperature rise under insignia  $b = 0$ .

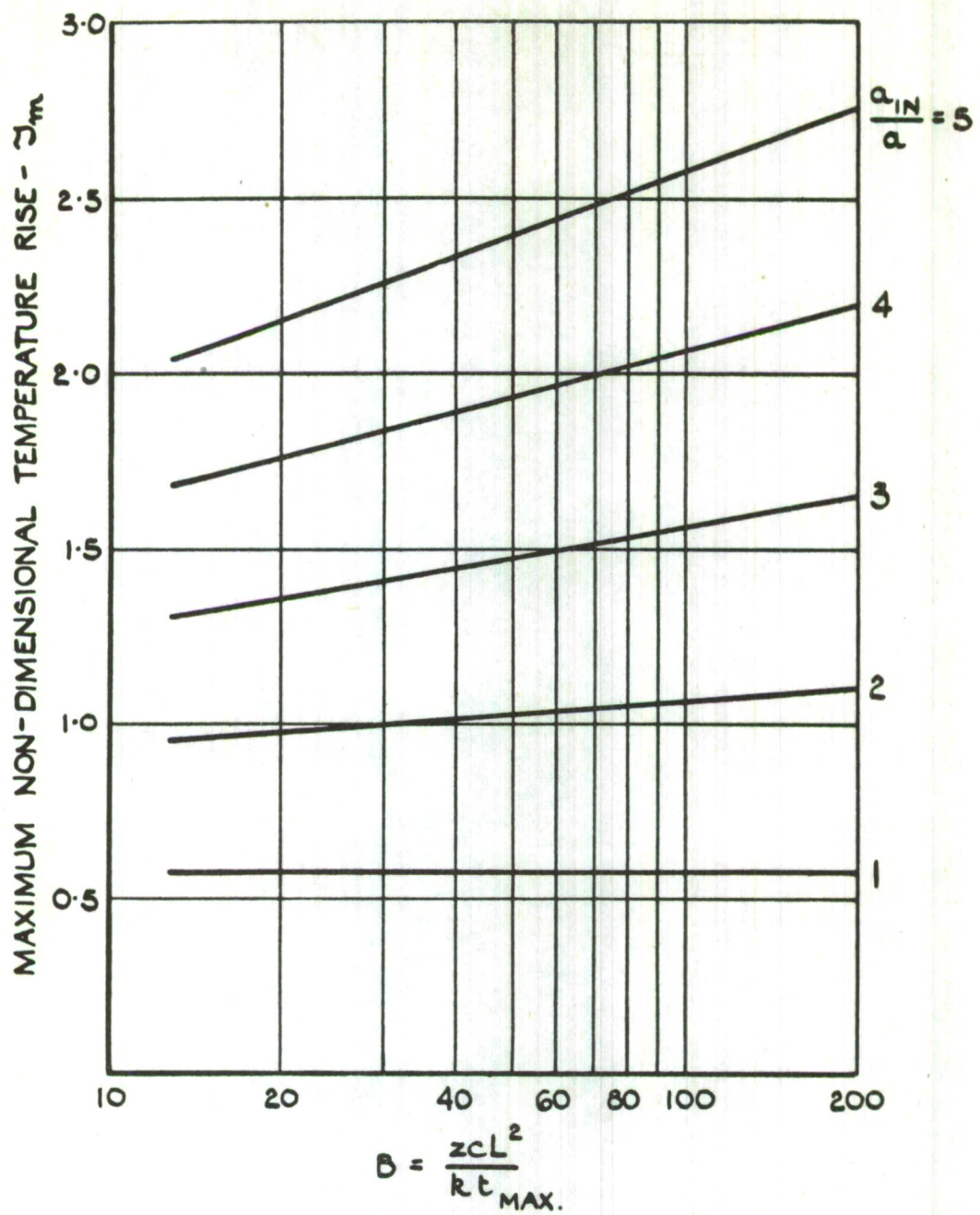


Fig. 5--Maximum temperature rise under insignia  $b = 0.08$ .



## DISTRIBUTION

### Military Distribution Categories 52 and 54

#### ARMY ACTIVITIES

- 1 Deputy Chief of Staff for Military Operations, D/A, Washington 25, D.C. ATTN: Dir. of SW&R
- 2 Chief of Research and Development, D/A, Washington 25, D.C. ATTN: Atomic Div.
- 3 Assistant Chief of Staff, Intelligence, D/A, Washington 25, D.C.
- 4 Chief of Engineers, D/A, Washington 25, D.C. ATTN: ENGTB
- 5-6 Chief of Ordnance, D/A, Washington 25, D.C. ATTN: ORDIN
- 7 Chief Signal Officer, D/A, Comb. Dev. and Ops. Div., Washington 25, D.C. ATTN: SIGCO-4
- 8 Chief of Transportation, D/A, Office of Planning and Int., Washington 25, D.C.
- 9-11 Commanding General, U.S. Continental Army Command, Ft. Monroe, Va.
- 12 Director of Special Weapons Development Office, Headquarters COMARC, Ft. Bliss, Tex. ATTN: Capt. Chester I. Peterson
- 13 President, U.S. Army Artillery Board, U.S. Continental Army Command, Ft. Sill, Okla.
- 14 President, U.S. Army Air Defense Board, U.S. Continental Army Command, Ft. Bliss, Tex.
- 15 President, U.S. Army Aviation Board, Ft. Rucker, Ala. ATTN: ATBG-DG
- 16 Commandant, U.S. Army Command & General Staff College, Ft. Leavenworth, Kansas. ATTN: ARCHIVES
- 17 Commandant, U.S. Army Air Defense School, Ft. Bliss, Tex. ATTN: Dept. of Tactics and Combined Arms
- 18 Commandant, U.S. Army Artillery and Missile School, Ft. Sill, Okla. ATTN: Combat Development Department
- 19 Commandant, U.S. Army Aviation School, Ft. Rucker, Ala.
- 20 Commandant, U.S. Army Ordnance School, Aberdeen Proving Ground, Md.
- 21 Commandant, U.S. Army Ordnance and Guided Missile School, Redstone Arsenal, Ala.
- 22 Commanding General, U.S. Army Chemical Corps, Research and Development Comd., Washington 25, D.C.
- 23-24 Commanding Officer, Chemical Warfare Lab., Army Chemical Center, Md. ATTN: Tech. Library
- 25 Commanding Officer, Diamond Ord. Fuze Labs., Washington 25, D.C. ATTN: Chief, Nuclear Vulnerability Br. (230)
- 26-27 Commanding General, Aberdeen Proving Grounds, Md. ATTN: Director, Ballistics Research Laboratory
- 28-29 Commanding Officer, Watervliet Arsenal, Watervliet, New York. ATTN: ORDBF-RR
- 30-31 Commanding General, U.S. Army Ord. Missile Command, Redstone Arsenal, Ala.
- 32 Commander, Army Rocket and Guided Missile Agency, Redstone Arsenal, Ala. ATTN: Tech Library
- 33 Commanding General, White Sands Proving Ground, Las Cruces, N. Mex. ATTN: ORDBS-OM
- 34 Commander, Army Ballistic Missile Agency, Redstone Arsenal, Ala. ATTN: ORDAB-HT
- 35 Commanding General, Ordnance Ammunition Command, Joliet, Ill.
- 36 Commanding General, USA Combat Surveillance Agency, 1124 N. Highland St., Arlington, Va.
- 37 Commanding Officer, USA Transportation R&E Comd., Ft. Eustis, Va. ATTN: Chief, Tech. Svcs. Div.
- 38 Commanding Officer, USA Transportation Combat Development Group, Ft. Eustis, Va.
- 39 Director, Operations Research Office, Johns Hopkins University, 6935 Arlington Rd., Bethesda 14, Md.
- 40 Commander-in-Chief, U.S. Army Europe, APO 403, New York, N.Y. ATTN: Opot. Div., Weapons Br.

#### NAVY ACTIVITIES

- 41 Chief of Naval Operations, D/N, Washington 25, D.C. ATTN: OP-03EG
- 42 Chief of Naval Operations, D/N, Washington 25, D.C. ATTN: OP-75
- 43 Chief of Naval Operations, D/N, Washington 25, D.C. ATTN: OP-922G1
- 44-45 Chief of Naval Research, D/N, Washington 25, D.C. ATTN: Code 811
- 46-47 Chief, Bureau of Aeronautics, D/N, Washington 25, D.C.
- 48-52 Chief, Bureau of Aeronautics, D/N, Washington 25, D.C. ATTN: AER-AD-41/20
- 53 Chief, Bureau of Ordnance, D/N, Washington 25, D.C.
- 54 Chief, Bureau of Ordnance, D/N, Washington 25, D.C. ATTN: S.P.
- 55 Director, U.S. Naval Research Laboratory, Washington 25, D.C. ATTN: Mrs. Katherine H. Cass
- 56-57 Commander, U.S. Naval Ordnance Laboratory, White Oak, Silver Spring 19, Md.
- 58 Director, Material Lab. (Code 900), New York Naval Shipyard, Brooklyn 1, N.Y.
- 59 Commanding Officer, U.S. Naval Mine Defense Lab., Panama City, Fla.
- 60-61 Commanding Officer, U.S. Naval Radiological Defense Laboratory, San Francisco, Calif. ATTN: Tech. Info. Div.
- 62 Commanding Officer, U.S. Naval Schools Command, U.S. Naval Station, Treasure Island, San Francisco, Calif.
- 63 Superintendent, U.S. Naval Postgraduate School, Monterey, Calif.
- 64 Commanding Officer, Nuclear Weapons Training Center, Atlantic, U.S. Naval Base, Norfolk 11, Va. ATTN: Nuclear Warfare Dept.
- 65 Commanding Officer, Nuclear Weapons Training Center, Pacific, Naval Station, San Diego, Calif.
- 66 Commanding Officer, U.S. Naval Damage Control Tng. Center, Naval Base, Philadelphia 12, Pa. ATTN: ABC Defense Course
- 67 Commanding Officer, Air Development Squadron 5, VX-5, China Lake, Calif.
- 68 Director, Naval Air Experiment Station, Air Material Center, U.S. Naval Base, Philadelphia, Pa.
- 69 Commander, Officer U.S. Naval Air Development Center, Johnsville, Pa. ATTN: NAS, Librarian
- 70 Commanding Officer, Naval Air Sp. Wpns. Facility, Kirtland AFB, Albuquerque, N. Mex.
- 71 Commander, U.S. Naval Ordnance Test Station, China Lake, Calif.
- 72-75 Commandant, U.S. Marine Corps, Washington 25, D.C. ATTN: Code A03H
- 76 Commanding Officer, U.S. Naval CIC School, U.S. Naval Air Station, Glynco, Brunswick, Ga.

#### AIR FORCE ACTIVITIES

- 77 Assistant for Atomic Energy, HQ, USAF, Washington 25, D.C. ATTN: DCS/O
- 78 Deputy Chief of Staff, Operations HQ, USAF, Washington 25, D.C. ATTN: Operations Analysis
- 79-80 Assistant Chief of Staff, Intelligence, HQ, USAF, Washington 25, D.C. ATTN: AFCIN-3B
- 81 Director of Research and Development, DCS/D, HQ, USAF, Washington 25, D.C. ATTN: Guidance and Weapons Div.
- 82 The Surgeon General, HQ, USAF, Washington 25, D.C. ATTN: Bio.-Def. Pre. Med. Division
- 83 Commander-in-Chief, Strategic Air Command, Offutt AFB, Neb. ATTN: OAWS



# CONFIDENTIAL

84	Commander, Tactical Air Command, Langley AFB, Va. ATTN: Doc. Security Branch	136-138	University of California Lawrence Radiation Laboratory, P.O. Box 808, Livermore, Calif. ATTN: Clovis G. Craig
85	Commander, Air Defense Command, Ent AFB, Colorado. ATTN: Atomic Energy Div., ADLAN-A	139	Argonne National Laboratory, P.O. Box 299, Lemont, Ill. ATTN: Dr. Hoylande D. Young
86	Commander, Air Force Ballistic Missile Div. HQ. ARDC, Air Force Unit Post Office, Los Angeles 45, Calif. ATTN: WDSOT	140-141	Bettis Plant, U.S. Atomic Energy Commission, Bettis Field, P.O. Box 1468, Pittsburgh 30, Penn. ATTN: V. Sternberg
87	Commander, Hq. Air Research and Development Command, Andrews AFB, Washington 25, D.C. ATTN: RDRWA	142-143	E. I. du Pont de Nemours and Co., Savannah River Laboratory, Document Transfer Station 703-A, Aiken, S.C.
88-89	Commander, AF Cambridge Research Center, L. G. Hanscom Field, Bedford, Mass. ATTN: CR&ST-2	144-145	General Electric Co., Aircraft Nuclear Propulsion Department, P.O. Box 132, Cincinnati 15, Ohio. ATTN: J. W. Stephenson
90-94	Commander, Air Force Special Weapons Center, Kirtland AFB, Albuquerque, N. Mex. ATTN: Tech. Info. & Intel. Div.	146-148	General Electric Co., P.O. Box 100, Richland, Wash. ATTN: M. G. Freidank
95-96	Director, Air University Library, Maxwell AFB, Ala.	149	U.S. Atomic Energy Commission, Hanford Operations Office, P.O. Box 550, Richland, Wash. ATTN: Technical Information Library
97	Commander, Lowry AFB, Denver, Colorado. ATTN: Dept. of Sp. Wpns. Tng.	150	Holmes and Narver, Inc., 828 S. Figueroa St., Los Angeles 17, Calif. ATTN: Sherwood B. Smith, Chief Project Engineer
98	Commandant, School of Aviation Medicine, USAF, Randolph AFB, Tex. ATTN: Research Secretariat	151	Knolls Atomic Power Laboratory, P.O. Box 1072, Schenectady, N.Y. ATTN: Document Librarian
99	Commander, 1009th Sp. Wpns. Squadron, Hq. USAF, Washington 25, D.C.	152	Lovelace Foundation, 4800 Gibson Boulevard, Albuquerque, N. Mex. ATTN: Dr. Clayton S. White, Director of Research
100-102	Commander, Wright Air Development Center, Wright-Patterson AFB, Dayton, Ohio. ATTN: WCOSI	153	National Lead Company of Ohio, P.O. Box 158, Mt. Healthy Station, Cincinnati 31, Ohio. ATTN: Reports Library
103-104	Director, USAF Project RAND, VIA: USAF Liaison Office, The RAND Corp., 1700 Main St., Santa Monica, Calif.	154	U.S. Atomic Energy Commission, New York Operations Office, 376 Hudson St., New York 14, N.Y. ATTN: Reports Librarian
105	Commander, Air Defense Systems Integration Div., L. G. Hanscom Field, Bedford, Mass. ATTN: SIDE-S	155-156	Phillips Petroleum Co., NRTS Technical Library, P.O. Box 1259, Idaho Falls, Idaho
106	Chief, Ballistic Missile Early Warning Project Office, 220 Church St., New York 13, N.Y. ATTN: Col. Leo V. Skinner, USAF	157	Chief, Radiological Health Branch, Office of Chief of Engineering Services, U.S. Public Health Service, Department of Health, Education and Welfare, Rm. 3072, North Building, 4th and C Streets, S.W., Washington 25, D.C. ATTN: James G. Terrill, Jr.
107	Commander, Air Technical Intelligence Center, USAF, Wright-Patterson AFB, Ohio. ATTN: AFCIN-4Bla, Library	158	U.S. Atomic Energy Commission, San Francisco Operations Office, 518 17th St., Oakland 12, Calif. ATTN: Technical Operations Div.
108	Assistant Chief of Staff, Intelligence, Hq. USAFE, APO 633, New York, N.Y. ATTN: Directorate of Air Targets	159-160	Union Carbide Nuclear Co., ORGDP Records Department, P.O. Box P, Oak Ridge, Tenn.
109	Commander-in-Chief, Pacific Air Forces, APO 953, San Francisco, Calif. ATTN: PFCIE-MB, Base Recovery	161-163	Union Carbide Nuclear Co., X-10 Laboratory Records Department, P.O. Box X, Oak Ridge, Tenn.
OTHER DEPARTMENT OF DEFENSE ACTIVITIES			
110	Director of Defense Research and Engineering, Washington 25, D.C. ATTN: Tech. Library	164	University of California at Los Angeles, Atomic Energy Project, P.O. Box 24164, West Los Angeles 24, Calif. ATTN: Thomas G. Hennessy, M.D.
111	Director, Weapons Systems Evaluation Group, Room 1E880, The Pentagon, Washington 25, D.C.	165-166	University of California Lawrence Radiation Laboratory, Technical Information Div., Berkeley 4, Calif. ATTN: Dr. R. K. Wakerling
112-119	Chief, Defense Atomic Support Agency, Washington 25, D.C.	167	University of Rochester, Atomic Energy Project, P.O. Box 287, Station 3, Rochester 20, N.Y. ATTN: Technical Report Control Unit
120	Commander, Field Command, DASA, Sandia Base, Albuquerque, N. Mex.	168	Reynolds Electrical & Engineering Co., Inc., P.O. Box 352, Las Vegas, Nev. ATTN: Mrs. Elizabeth E. Heyer and Mrs. Gertrude M. Schroer
121	Commander, Field Command, DASA, Sandia Base, Albuquerque, N. Mex. ATTN: FCTG	169	Weapon Data Section, Technical Information Service Extension, Oak Ridge, Tenn.
122-123	Commander, Field Command, DASA, Sandia Base, Albuquerque, N. Mex. ATTN: FCWT	170-200	Technical Information Service Extension, Oak Ridge, Tenn. (surplus)
124	Administrator, National Aeronautics and Space Administration, 1520 "H" St., N.W., Washington 25, D.C. ATTN: Mr. R. V. Rhode		
125	U.S. Documents Officer, Office of the United States National Military Representative - SHAPE, APO 55, New York, N.Y.		
ATOMIC ENERGY COMMISSION ACTIVITIES			
126-128	U.S. Atomic Energy Commission, Technical Library, Washington 25, D.C. ATTN: For IMA		
129-130	Los Alamos Scientific Laboratory, Report Library, P.O. Box 1663, Los Alamos, N. Mex. ATTN: Helen Redman		
131-135	Sandia Corporation, Classified Document Division, Sandia Base, Albuquerque, N. Mex. ATTN: H. J. Smyth, Jr.		